



Multifaceted applications of isolated microalgae *Chlamydomonas* sp. TRC-1 in wastewater remediation, lipid production and bioelectricity generation



Kannikka Behl^a, Pasupuleti SessaCharan^a, Monika Joshi^b, Mahima Sharma^b, Ashish Mathur^b, Mukul Suresh Kareya^c, Pannaga Pavan Jutur^c, Amit Bhatnagar^d, Subhasha Nigam^{a,*}

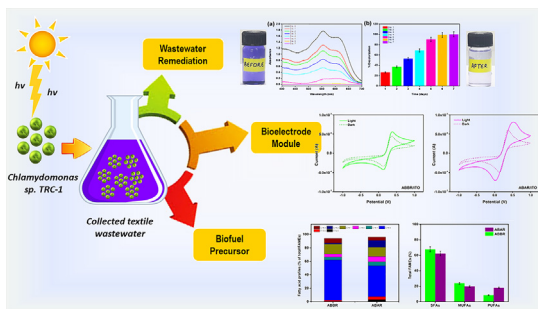
^a Amity Institute of Biotechnology, Amity University, Noida, Uttar Pradesh 201313, India

^b Amity Institute of Nanotechnology, Amity University, Noida, Uttar Pradesh 201313, India

^c Omics of Algae Group, Integrative Biology, International Centre for Genetic Engineering and Biotechnology, New Delhi 110067, India

^d Department of Environmental and Biological Sciences, University of Eastern Finland, P. O. Box 1627, FI-70211, Kuopio, Finland

GRAPHICAL ABSTRACT



ARTICLE INFO

Keywords:

Biofuels
Bioremediation
Electrogenic
Microalga
Textile effluent

ABSTRACT

Green microalga, *Chlamydomonas* sp. TRC-1 (*C. TRC-1*), isolated from the outlet of effluent treatment plant of textile dyeing mill, was investigated for its competence towards bioremediation. Algal biomass obtained after remediation (ABAR) was implied for bioelectricity and biofuel production. *C. TRC-1* could completely decolorize the effluent in 7 days. Significant reduction in pollution-indicating parameters was observed. Chronoamperometric studies were carried out using cyclic voltammetry and electrochemical impedance spectroscopy (EIS). Maximum current density, power and power density of 3.6 A m^{-2} , $4.13 \times 10^{-4} \text{ W}$ and 1.83 W m^{-2} , respectively were generated in ABAR. EIS studies showed a decrease in resistance of ABAR, supporting better electron transfer as compared to algal biomass before remediation (ABBR). Its candidature for biofuel production was assessed by estimating the total lipid content. Results revealed enhancement in lipid content from 46.85% (ABBR) to 79.1% (ABAR). Current study advocates versatile potential of isolated *C. TRC-1* for bioremediation of wastewater, bioelectricity production and biofuel generation.

1. Introduction

Dye containing colored wastewater released from textile industries

causes serious environmental pollution due to occurrence of toxic organic and inorganic contaminants (Huy et al., 2018). Therefore, prior to discharge into water reservoirs it is obligatory to treat them properly to

* Corresponding author.

E-mail address: snigam@amity.edu (S. Nigam).

<https://doi.org/10.1016/j.biortech.2020.122993>

Received 8 December 2019; Received in revised form 2 February 2020; Accepted 7 February 2020

Available online 11 February 2020

0960-8524/ © 2020 Elsevier Ltd. All rights reserved.

avoid harmful effects on aquatic and terrestrial ecosystems.

Most textile industries are equipped with effluent treatment plants (ETPs) that cleanses industrial effluents. However, despite being treated, the released effluent still does not meet the pollution criteria set up by environment protection authorities (Qie et al., 2019).

Although several physical and chemical methods are employed for effluent treatment, they inherit disadvantages such as low removal efficiency, generation of high amount of sludge and high operational costs (Huang et al., 2019). An alternative approach utilizing microbes (bacteria, fungi and microalgae) for bioremediation can prove to be efficient, eco-friendly and cost effective. However, heterotrophic microbial cultures (bacteria and fungi) require a specific media with additional carbon sources for their growth, generating toxic compounds in the sludge and increasing the maintenance cost (Ahmad et al., 2018). In recent years, utilization of microalgae in bioremediation of textile effluents has garnered attention owing to their ability of quick acclimatization as well as nutrient and CO₂ assimilation. Photoautotrophic microalgal bioremediation is faster, cost effective and sustainable as compared to heterotrophic microbial cultures and is also beneficial in terms of non-pathogenicity (Aragaw & Asmare, 2018). Microalgae can convert azo dyes into simpler compounds using inducible enzymes such as superoxide dismutase and azo reductase that reduce the azo bond (N=N) of dye into aromatic amines (-NH₂) (Behl et al., 2019a). In addition, biosorption of contaminants on the algal cell wall is due to its cell wall structure, which is ornamented by diverse functional groups acting as binding sites (Sinha et al., 2016).

The spent-biomass rich in C16 and C18 fatty acids can be used as feed-stock for biofuel production (Behl et al., 2019a). In addition to the biofuel production, microalgae have been gaining considerable importance in the area of bioelectrode fabrication as a conducting material for microbial fuel cells (MFC), applications that can convert solar energy into bioelectricity through biomass (Ge & Champagne, 2017).

In the present study, a newly isolated *Chlamydomonas* sp. TRC-1 (*C. TRC-1*) was used for bioremediation of textile effluent. The aim of the study was to investigate (i) the biomass and metabolite production of *Chlamydomonas* sp. TRC-1 cultivated in effluent, (ii) utilization of lipid as a biofuel precursor and (iii) feasibility of the algal based electrodes towards photocurrent generation. Optimized performances of the microalgae in effluent remediation were evaluated in algal biomass before (ABBR) and after remediation (ABAR) in terms of pollution-indicating parameters. Biochemical components such as carbohydrates, and proteins were probed. Lipids were extracted from the microalgal biomass and fatty acid profiles were analyzed for biodiesel production. Furthermore, electrochemical studies were also performed for ABBR and ABAR to investigate its ability for bioelectricity generation. The aforementioned investigations, thus, revealed that the one-time cultivated *Chlamydomonas* sp. TRC-1 in effluent has tremendous potential to be used in versatile applications towards environmental sustainability even after remediation.

2. Materials and methods

2.1. Chemicals

Analytical grade sodium hydroxide (NaOH), hydrochloric acid (HCl), sodium chloride (NaCl), methanol, sodium carbonate (Na₂CO₃), copper sulphate (CuSO₄), sodium-potassium tartrate (K-Na-C₄H₄O₆·4H₂O), mercuric chloride (HgCl₂), potassium iodide (KI), sulphuric acid (H₂SO₄), phenol, chloroform, ammonium chloride (NH₄Cl), hexane, deionized water, silver chloride (AgCl), ferric chloride (FeCl₃) potassium chloride (KCl), potassium ferricyanide (K₃Fe(CN)₆), and potassium ferrocyanide (K₄Fe(CN)₆·3H₂O) were obtained from Sigma-Aldrich. ITO electrodes were purchased from Techinstro India, had a thickness of 2.3 mm, with about 7 Ω/sq. surface resistivity. BG-11 medium was also used for algal cultivation.

2.2. Effluent collection

The effluent for experiment was stored from the outlet of an ETP of dye bath industry located at Faridabad-Ballabgarh, Haryana, India and labelled as FTE (Faridabad Textile Effluent). Since the textile dye bath industry involves dyeing fabrics with different colours of chemical dyes; the generated effluent consists of hydrolysed unfixed dyes, surfactants, salts, sulphides, and heavy metals in an alkaline medium. Samples were collected in sterile polypropylene bottles labelled and preserved as per standard methods (Rice et al., 2012).

2.3. Isolation and identification of microalgal species

Chlamydomonas sp. TRC-1 (Accession no: MF162271), a unicellular microalga (green) was isolated from FTE, serially diluted and incubated in growth chambers (26 °C; 16:8 h light: dark cycle; 100 μmol photons m⁻² s⁻¹) in nutrient rich BG-11 medium. Axenic cultivation of the isolate was further conducted to attain sufficient algal biomass as an inoculum for further experimental studies.

2.4. Biomass analysis

2.4.1. Growth rate studies

Cell growth was estimated by determining the dry cell weight (DCW). Growth rate was monitored in both commercially available BG-11 and FTE. Optical density (OD) at 680 nm was observed and values were converted to DCW (g L⁻¹) (Daneshvar et al., 2018b). The correlation between the dry cell weight (DCW) of microalga and OD was monitored using Eq. (1):

$$DCW(g L^{-1}) = a \times OD_{680} - b \quad (1)$$

where, OD₆₈₀ is the optical density of microalga at 680 nm and *a* and *b* are the constants. Specific growth rate (S.G.R.) and productivity (P) of the algal biomass was calculated for the time period of the highest increase in culture biomass concentration (Daneshvar et al., 2018b; Han et al., 2016).

2.4.1.1. Chlorophyll *a* fluorescence transient measurements. Chlorophyll *a* fluorescence signals were recorded at room temperature using the Dual-PAM-100 fluorometer (Heinz Walz, Effeltrich, Germany). Samples were dark adapted for 30 min to allow complete oxidation of all the reaction centres. A saturation light pulse (6000 μmol photons m⁻² s⁻¹; λ = 660 nm) was used to determine the *F_m* value. Maximum photochemical efficiency of PSII (*F_v/F_m* = (*F_m* - *F_o*)/*F_m*) was then calculated (Agarwal et al., 2018). Quantum yields of photochemical quenching, Y (II); non-photo-chemical quenching, Y (NPQ); and the energy dissipated as heat or fluorescence, Y (NO), were calculated from the fluorescence values obtained. The PSII operating efficiency was calculated as described previously by Baker (*F_q'/F_m'*) (Baker, 2008). Samples for analysis in biological triplicates (n = 3) were aliquoted on 0th, 7th and 14th day with chlorophyll concentration of 40 μg mL⁻¹ before the measurements.

2.5. Bioremediation studies: effluent characterization and removal efficiency

FTE was characterized for physicochemical parameters and evaluated for degradation after microalgal treatment. The concentration of colour, pH, BOD, COD, TSS, TDS, TS, nitrate (NO₃-N), total nitrogen, and phosphate content, hardness were analysed on the first and the final day of the bioremediation experiment using standard APHA protocols (Rice et al., 2012). The COD of algal biomass (ABBR/ABAR) was measured according to standard APHA protocols (Rice et al., 2012). Decolorization experiments were also performed simultaneously. A control containing no algal population with FTE was also run parallel to assess the degradation by photolysis. FTE samples were centrifuged at

5000 rpm at regular time intervals to pellet down the cell mass and absorbance of the supernatant was evaluated. Percent reductions of parameters were calculated by the following Eq. (2):

$$\text{Pollution parameter reduction(\%)} = \frac{x_i - x_f}{x_i} \times 100 \quad (2)$$

where, x_i is initial concentration and x_f is final concentration after the remediation.

Adsorption and/or biodegradation are main phenomenon for microbial decolorization (Wu et al., 2012). Plausible FTE mechanisms for decolorization (adsorption or biodegradation) were assessed using sodium azide (NaN_3) treatment. Addition of metabolic inhibitor NaN_3 (0.50 g in 50 mL of 0.4 OD algal cells) confirmed the decolorization only by adsorption process through cell wall. Further, for the validation, 2, 3, 5-triphenyltetrazolium chloride (TTC) was conducted for the evaluation of cell viability (Sinha et al., 2016).

2.6. Biochemical composition

Total proteins were extracted and analysed following the modified method of Rausch (1981) and was determined by Bradford method (Bradford, 1976). Phenol-sulphuric acid technique was used for the determination of carbohydrate (total) (Salama et al., 2014).

Total lipid content was obtained from the algal biomass using a slightly modified Bligh and Dyer method (Bligh and Dyer, 1959). Esterification of lipid extract was done under acidic condition using the methodology of Francisco et al. (2010). For gas chromatography-mass spectroscopy (GC-MS) analysis the methyl esters were dissolved in hexane. FAMES composition was investigated using a GC attached with a split automatic injector and silica capillary column on Rtx-5. As a carrier gas Helium was used (flow rate 1 mL min⁻¹). The operational temperature of the column was 140 °C for 1 min and ramped to 260 °C with an increasing rate of 30 °C min⁻¹. The experiment was conducted at 280 °C (15 min). The results were compared and confirmed with standards.

2.7. Electrochemical analysis: cyclic voltammetry (CV) and electrochemical impedance spectroscopy (EIS)

To understand the electrochemical activity of the *C. TRC-1*, before and after remediation, CV studies were performed using *Auto lab PGSTAT-10*, a three-electrode electrochemical workstation using ITO, Ag/AgCl and platinum wire as working, reference and counter electrodes respectively. CV scans were measured between -1.0 V to 1.0 V potential (scan rate of 100 mV s⁻¹) in KCl solution (pH 3.2; 0.1 M; containing 5 mM Fe (CN)₆^{3-.4-}) as the electrolyte source. EIS measurements were performed on a potentiostat/galvanostat (Multiautolab (MA204), Autolab, Netherlands) workstation using the similar setup. The Current density, power and power density were calculated from the following formula previously described by Fong-Lee Ng (Ng et al., 2017). For bioelectrode fabrication, *C. TRC-1* were grown for 10 days on ITO electrode under visible light. Algal biofilm was prepared by placing on ITO electrodes in exponential phase culture (0.4 OD, 100 mL) of ABBR and ABAR and illuminated at 1500 lx. To find if extracellular electron transfer occurred via direct or indirect mechanism, an anaerobic environment was provided. During experiments, nitrogen gas was used for 35 min to the electrolyte buffer.

2.8. Scale up studies for large scale bioremediation

An experimental setup consisting of (a) effluent container, (b) treatment chamber and (c) collection reservoir was constructed to investigate the feasibility of the microalgal isolate for large scale bioremediation. The treatment chamber was 14 cm in diameter and 20 cm in height. Treatment chamber was equipped with agitation, temperature, pH controls and a pump for aeration. Bioremediation studies were

performed in the treatment chamber filled with FTE and algal beads (1 OD) under 100 μmol photons m⁻² s⁻¹ light intensity. FTE was recycled until complete decolorization and finally collected in collection reservoir via a steady flow rate (5 mL min⁻¹). Optimized experimental conditions were: operational volume: 2000 mL, temperature: 27 ± 2 °C; pH: 10; algal beads (1 OD); agitation: 35–40 rpm. A residence time of 6.67 h was provided before FTE was collected for decolorization and bioremediation evaluation. Dilution rate and residence time were estimated using the formulae previously described by El-Batal et al. (2012). The performance of the experimental set-up was evaluated on the basis of amount of COD removed (COD_{rem}) during the process. COD removal was calculated by fitting the experimental data in COD mass balance equation (3):

$$\text{COD}_{\text{rem}}(\%) = \text{COD}_{\text{BT}} + \text{COD}_{\text{Algal biomass}} - \text{COD}_{\text{AT}} \quad (3)$$

where COD_{BT} and COD_{AT} are concentration of COD (mg L⁻¹) before and after bioremediation. COD_{Algal biomass} is the concentration of COD of the algal biomass.

3. Results and discussions

3.1. Growth studies

Textile effluent induces a natural selective stress on the growth of specific microalga with certain characteristics. BG-11 and FTE were used as source of growth media for feasibility of *C. TRC-1* growth with an initial cell density of 0.8039 g L⁻¹ (DCW) (Fig. 1a). A significant change in the growth behaviour was obtained for *C. TRC-1* cells growing in the two media. Cells grown in BG-11 exhibited: (a) increase in growth with maximum growth attained at day 13 (DCW: 3.3 g L⁻¹), (b) steady growth (day 13–14) and (c) decrease in growth from day 15 onwards. Cells grown in BG-11 had a SGR of 0.124 g d⁻¹ and recorded a biomass productivity of 0.14 g L⁻¹ d⁻¹. While for *C. TRC-1* cells cultivated in FTE displayed: (a) increase in growth with maximum growth attained at day 7 (DCW: 2.49 g L⁻¹), (b) steady growth (day 7–8) and (c) decrease in growth from day 8 onwards. Cells cultivated in FTE recorded an SGR of 0.188 g d⁻¹ and biomass productivity of 0.28 g L⁻¹ d⁻¹. It was quite interesting to note that FTE showed rapid and higher growth till 7 days (DCW: 2.49 g L⁻¹) as compared to BG-11 (DCW: 1.695 g L⁻¹). However, FTE did not support the growth beyond 8 days.

FTE is a complex medium including high contents of BOD, COD, organic and inorganic and nitrogen compounds. Higher biomass production at can be related to the nutrients present FTE. Additionally, the transient stimulation of growth may be attributed to production of various metabolites by *C. TRC-1* as its survival strategy. The results are in agreement with Asthana et al. (2005). Literature review also indicates that microalgae can grow well in wastewaters as they have the ability to utilize inorganic nitrogen and phosphorous compounds present in the effluent (Ji et al., 2014). Therefore, this encouraged us to investigate the feasibility of ABAR for bioenergy production.

3.2. Chlorophyll-a content and photosynthetic capacity of *C. TRC-1*

In this study, we measured the Chl a fluorescence for the strain *Chlamydomonas* sp. *TRC-1* grown in FTE and culture media (BG-11). Maximum quantum efficiency of PSII photochemistry (F_v/F_m) of the samples associated to cultures grown in FTE showed an increase of approximately 12% until the 7th day as compared to the control (Fig. 1b). This indicates that the photosynthetic machinery of the treated cells is highly active initially as compared to the control, enhancing the doubling time of cells i.e., growth rate with no limitation of nutrients grown in the effluent dye. However, the F_v/F_m ratio changes drastically by the 14th day, demonstrating the decrease in cell growth rate in the treated cells to approximately 28% as compared to the 7th day. On the other hand, cells grown in BG-11 showed an increase in

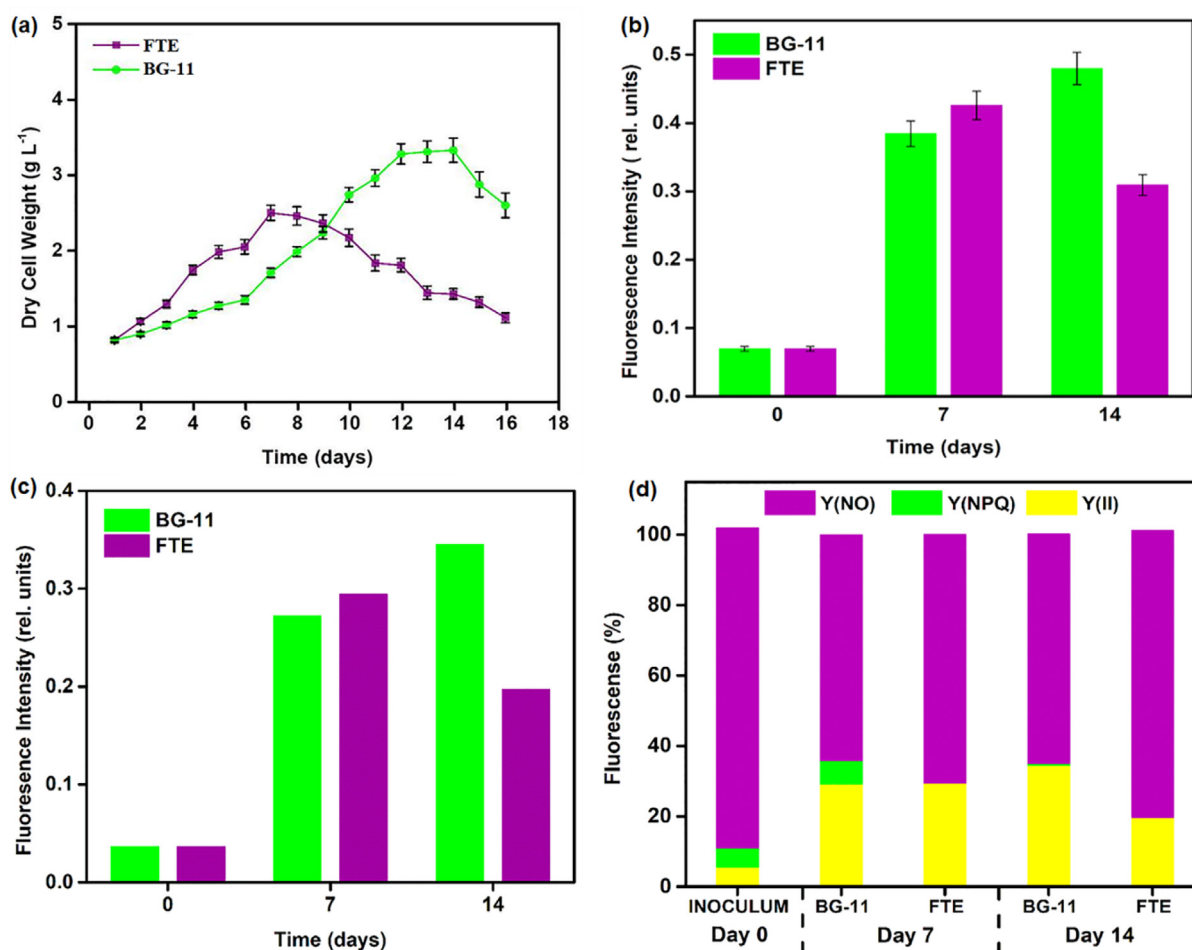


Fig. 1. (a) Growth profiles of *C. TRC-1* cultivated in commercially available growth medium (BG-11) and Faridabad Textile Effluent (FTE) for 16 days. (b) Bar diagram indicating maximum quantum efficiency of PSII photochemistry i.e., F_v/F_m for BG-11 (green) and FTE (violet) cultivated *C. TRC-1* cells. (c) Bar diagram indicating the PSII operating efficiency i.e., the F_q'/F_m' ratio for BG-11 (green) and FTE (violet) cultivated *C. TRC-1* cells. (d) Quantum yields of photochemical quenching (Y (II) represented in yellow bars), non-photochemical quenching (Y (NPQ) represented in green bars) and the non-light induced energy dissipated as heat or fluorescence (Y (NO) represented in purple bars) for BG-11 and FTE cultivated *C. TRC-1* cells. (For interpretation of the references to colour in this figure legend, the reader is referred to the web version of this article.)

their F_v/F_m , increasing approximately 20% as compared to the 7th day. This indicates that the light absorbed by the effluent-grown cells that was used in photosynthesis decreases after 7th day. Fig. 1c illustrates the graph for the PSII operating efficiency, which provides an estimate of the quantum yield of linear electron flux through the PSII. It is in correlation with the quantum efficiency of the PSII photochemistry, also showing a similar pattern to the growth curve. We can see in Fig. 1c that the effluent-grown cells had a higher operating efficiency at 7th day as compared to the control, however, its efficiency decreased with time, indicating that the cells might have been in continuous stress once the nutrients are limited after the 7th day.

Our study also suggests that the electron flow in the cells grown in FTE followed the Z-scheme during the initial phase of its growth (i.e., 1–7th day), wherein it accumulated the reducing power, NADPH, and ATP. On the contrary, at the latter time intervals (after 7th day), due to increased stress and limited nutrients, we can assume that the electron flow in the cells switched from non-cyclic photophosphorylation to cyclic mode of photophosphorylation in which it utilizes energy accumulated in the initial stage of its growth to compensate the cellular metabolism. In the present study, Fig. 1d illustrates the Y (II), Y (NPQ), and Y (NO). The quantum yield of PSII Y (II), of both control and effluent-grown cells were comparable at 7th day, however, Y (II) values declined considerably for FTE-grown cells after 14th day and was in strong correlation to Fig. 1a–c. It was evident from Fig. 1d that the

energy dissipation through Y (NO) kept on increasing for FTE-grown cells till the 14th day. Y (NO) is often described as a simple indicator of the reduction state of plastoquinones within the photosynthetic membranes. Under exposure to high irradiances, plants and algae are known to minimize the reduction state of these plastoquinones (Agarwal et al., 2018). As a result, we can say that FTE treated cells were quite successful in regulating the photosynthetic electron transport chain compared to control.

3.3. Analysis of physicochemical parameters and nutrient removal

Considering the property of acclimatized algal biomass to survive and grow in textile effluents, *C. TRC-1* was tested for biodegradation and decolorization of FTE. Physicochemical parameters of the treated and untreated FTE were compared with the permissible limits provided by Central Pollution Control Board (CPCB), India and are summarized in Table 1. Reduction in pH from 10.9 to a stable 8.5 was observed after treatment which can be accredited to the reduction of CO₂ caused by photosynthesis of *C. TRC-1* (Ordoñez et al., 2019). Additionally, the alkaline conditions also rupture the algal cell wall, thereby exposing additional functional groups, which, in turn, enhances the removal efficiency (El-Naggar et al., 2018). *C. TRC-1* could also successfully reduced BOD (87.54%), from 765.5 mg L⁻¹ to 96 mg L⁻¹ after remediation, thereby reducing the toxicity level of FTE. A similar pattern

Table 1
Physicochemical parameters of FTE before and after incubation with isolated microalgae *C. TRC-1*.

Parameter	CPCB Permissible Limit*	Before Treatment	After Treatment (7 days)	Percent (%) Removal
Colour	Colourless	Violet	Colourless	–
pH	6.5–8.5	10.9 ± 0.54	8.5 ± 0.42	–
BOD (mg L ⁻¹)	30	765.5 ± 38.27	96 ± 8.8	87.54
COD (mg L ⁻¹)	250	1378.2 ± 68.90	316 ± 15.8	83.08
TDS (mg L ⁻¹)	100	8195 ± 409.75	1466 ± 73.3	82.11
TSS (mg L ⁻¹)	2000	1050 ± 52.5	138.2 ± 6.91	87.40
TS (mg L ⁻¹)	2100	9245 ± 462.25	1604.2 ± 80.21	82.64
Total nitrogen (mg L ⁻¹)	10–30	40 ± 1.0840	5.14 ± 0.892	87.15
Nitrate (mg L ⁻¹)	< 5	16.129 ± 2.58	1.33 ± 0.645	91.75
Phosphate (mg L ⁻¹)	< 10	2.1 ± 0.25	0.16 ± 0.05	92.36
Hardness (mg L ⁻¹)	200	168.38 ± 16.21	114 ± 6.3	32.29
Chloride (mg L ⁻¹)	200–1000	1019.46 ± 36.08	597 ± 4.8	41.43
Turbidity (NTU)	10	43.57 ± 1.53	12 ± 0.5	72.45
Alkalinity (mg L ⁻¹)	200–600	1162.66 ± 19.27	632 ± 5.41	45.64
CO ₂ content (mg L ⁻¹)	100	1200 ± 25.14	136 ± 6.2	88.66
Water stability	–	Corrosive	Stable	–

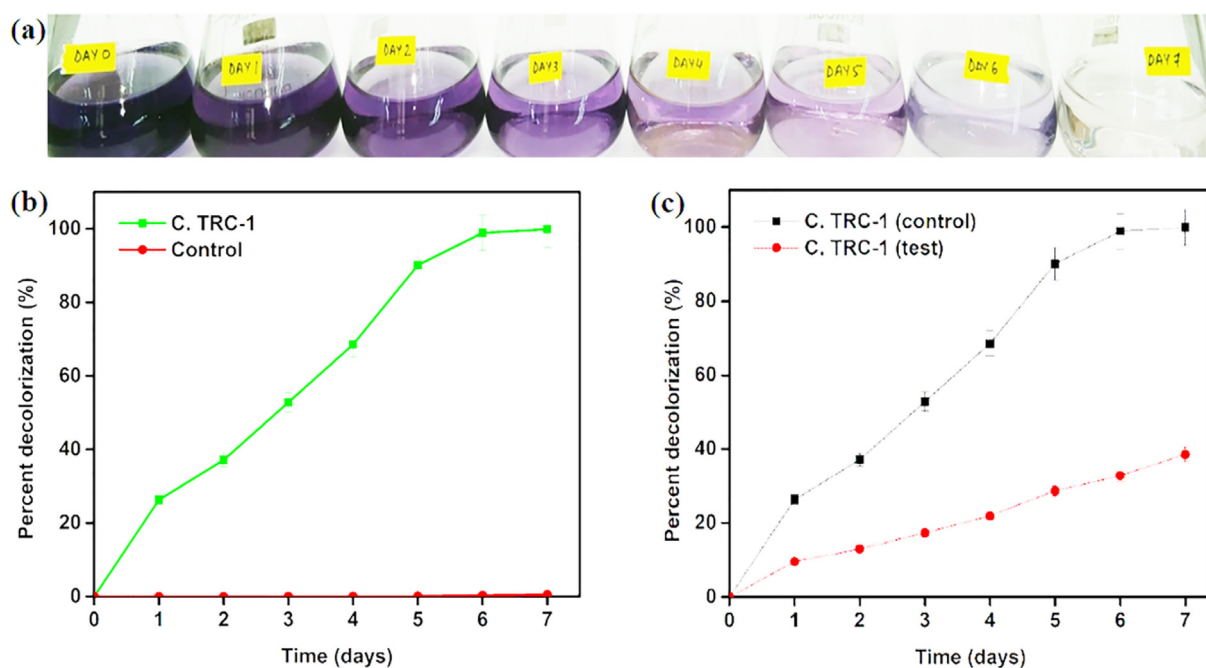


Fig. 2. (a) Pictorial visualization of FTE showing periodic decolorization by *C. TRC-1* till 7 days. (b) FTE degradation (%) by *C. TRC-1* under visible light irradiation (at $\lambda_{max} = 555 \text{ nm}$; $0.4 \text{ OD algal cells}$) in 50 mL and (c) Dye decolorization of FTE (40 mg L^{-1}) by *C. TRC-1* cells treated with NaNO_3 (0.1 g) (●, test) and without NaNO_3 (■, control).

was also observed for COD, where the final concentration (316 mg L^{-1}) was reduced after remediation, confirming the COD removal during the experiment. The algal biomass recorded a COD of 81 mg L^{-1} . A gradual decline in the COD was observed, which can be explained by the fact that the photosynthetic *C. TRC-1* produces oxygen that in turn enhances the biological degradation of the organic matter in FTE, thus accounting for both BOD and COD reduction (Gupta et al., 2019). Removal of TDS from 8195 mg L^{-1} to 1466 mg L^{-1} can be ascribed to the biosorption of *C. TRC-1* (Hwang et al., 2016). Reduction in hardness from 168 mg L^{-1} to 114 mg L^{-1} can be attributed to the precipitation of CaCO_3 by *C. TRC-1* for their growth (Subashini & Raju, 2018). Significant reduction in other parameters like TDS, TSS, EC, hardness and alkalinity may be due to the ability of the algal species to consume nutrients during algal growth (Aragaw & Asmare, 2018). Results reported by Yu states TDS as one of the essential factors that define the relationship of culture medium species in the cultivation of microalgae during nutrient removal (Yu et al., 2019).

Changes in Total nitrogen, nitrate ($\text{NO}_3\text{-N}$) and phosphate (PO_4^{3-})

concentrations were also monitored to understand the degradation of FTE and nutrient removal. It was observed that *C. TRC-1* removed 91.75% (1.33 mg L^{-1}) nitrate and 87.15% total nitrogen (5.14 mg L^{-1}) from FTE after complete decolorization (7 days). Microalgae can efficiently remove inorganic and organic forms of nitrogen from the wastewater, degrading/reducing complex nitrogen compounds into simpler forms by nitrate and nitrite reductase enzymes (Daneshvar et al., 2018b). Efficient nitrogen removal by *Scenedesmus quadricauda* (95%), *Scenedesmus abundans* (83%), *Chlorella pyrenoidosa* (87%) and *Chlamydomonas pyrenoides* (90%) from industrial effluents have been reported by various research groups (Daneshvar et al., 2018c). Higher nitrate removal efficiency could be attributed to the acclimatized species, as well as denitrification of nitrate and volatilization of ammonia (Guldhe et al., 2017). Relatively lower removal efficiency for total nitrogen can possibly be accredited to the presence of certain organic nitrogenous compounds which cannot be utilized by *C. TRC-1*.

The initial concentration of phosphate in FTE was observed as 2.1 mg L^{-1} , which was 92.36% removed after complete decolorization.

Inorganic phosphorous in the form of phosphate plays a pivotal role in algal growth and energy metabolism (Emparan et al., 2019). Research conducted by Martínez states that algal metabolism is mostly dependent on inorganic phosphorous (HPO_4^{2-} , H_2PO_4); which is converted into organic compounds leading to ATP production; and transferred across the algal cell for utilization (Martínez et al., 1999). Both nitrate and phosphate present in FTE are adsorbed through matrix pore surface of *C. TRC-1*. Further, uptake and assimilation of these inorganic compounds by the cells increase the algal growth. This results in reduction of nitrogen and phosphorous content in FTE, thereby improving the quality of water.

3.4. Plausible mechanism for FTE decolorization

It was observed that *C. TRC-1* was able to degrade 99.89% colour after 7 days in the present study (Fig. 2 a-b). Both adsorption and biodegradation are integral elements that partake in the dye decolorization process. This was further determined by treating *C. TRC-1* cells with and without NaN_3 treatment that investigated dominant mode of mechanism involved in dye removal. Decolorization studies were performed using 40 mg L^{-1} violet FTE solutions. (Fig. 2c). A significant removal efficiency of 99.89% was observed after 7 days for *C. TRC-1* cells cultivated without NaN_3 treatment (control), demonstrating that living algal cells displayed both adsorption and biodegradation processes for dye removal (Fig. 2c). However, after NaN_3 addition, the internal cellular metabolism ceased, leading to cell death and the dye removal occurred solely via bioadsorption (38.56%). Although both processes were cohesively involved in the dye removal, the dominant mode of dye decolorization was biodegradation (61.33%).

Efficient dye removal by *C. TRC-1* may be attributed to the accumulation of the dye ions on its surface and assimilation of the toxic chromophores inside the cell and its conversion into simpler, non-toxic compounds (Emparan et al., 2019). Additionally, studies conducted by Daneshvar et al. stated that removal of colour by microalgae occurred due to three inherently separate mechanisms of assimilative consumption of chromophores for the production of algal biomass, transformation of coloured molecules to non-coloured molecules, and adsorption of chromophores on algal biomass (Daneshvar et al., 2007). Dyes can be removed from effluent solutions either via physicochemical interactions (adsorption) and/or via the impact of metabolic-dependent processes (e.g. enzyme mediated degradation/decolorization) (Behl et al., 2019a). Bioconversion of azo dyes by algae into simpler compounds is brought about by the inducible enzyme, “azo reductase” which catalyses NAD(P)H dependent reduction of the azo bond ($\text{N}=\text{N}$) to aromatic amines ($-\text{NH}_2$), which are further degraded aerobically by *C. TRC-1* (Sinha et al., 2016).

3.5. Biochemical composition

Parameters like nutrient media composition, concentration and cultivation conditions are responsible for variations in growth pattern and the biochemical composition in microalgae. *C. TRC-1* biomasses were cultivated in BG-11 and FTE (ABAR) and investigated for their carbohydrate, lipid and protein content after complete decolorization of FTE (7 days) and is depicted in Fig. 3a. The total percentage of accumulated carbohydrate for *C. TRC-1* cells cultivated in BG-11 medium increased from 7% (ABBR) to 16% after 7 days of cultivation, whereas, it was recorded as 19.5%, when *C. TRC-1* cells were cultivated in FTE. The carbohydrates accumulated by the microalga can be transformed into fermentable sugars and utilized as appropriate bioresources in bioethanol production. Some *Chlamydomonas* species can produce more carbohydrates under certain conditions. High concentrations of phosphorous and nitrogen present in FTE could have contributed to the enhancement of protein content when *C. TRC-1* cells were cultivated in it (Acién Fernández et al., 2018). These results are in accordance with studies conducted by Daneshvar et al. (2018a). The maximum protein

content was observed in *C. TRC-1* cells cultivated in FTE (51.9%) as compared to *C. TRC-1* cells cultivated in BG-11 medium (33.6%) after 7 days of incubation. Corroborating with the results obtained in the current study, a similar range of concentration of protein was noted for control and experimental analysis by different research groups (Daneshvar et al., 2018a).

C. TRC-1 biomasses (ABBR/ABAR) were investigated for their lipid content and productivity after complete decolorization of FTE (7 days). Under the above-mentioned experimental growth conditions, the total lipid content was observed as 7% for ABBR and 11% for ABAR of their respective dry cell weight and the difference was statistically significant (p value < 0.00001) for ABAR (Fig. 3a). Lipid productivity after complete FTE decolorization was observed as 0.17 g $\text{L}^{-1} \text{d}^{-1}$ and 0.38 g $\text{L}^{-1} \text{d}^{-1}$ for ABBR and ABAR respectively. Some *Chlamydomonas* species can produce more lipids under certain conditions (Xu et al., 2018). Higher amount of lipid content and production of ABAR could be attributed to the growth behaviour of *C. TRC-1* cells in FTE at day 7, when the stationary phase begins (Fig. 1a). As *C. TRC-1* attained its stationary phase, it had utilized its food reserves for its growth and now accumulated lipids for its endurance. The finding of this result is hand in hand with Nigam et al. (2011). An enhancement in the biochemical composition of *C. TRC-1* cells cultivated in BG-11 from 18.6% to 56.6% was recorded after 7 days of cultivation; which increased to 82.5% when cultivated in FTE as a nutrient media (Fig. 3a). Textile dye bath effluents (such as FTE) are rich in nutrients like phosphorous, nitrogen and have excessive carbon content. Possessing a high nutrient content makes them a potential candidate for simultaneous microalgal cultivation and achieving high biomass yield and lipid productivity for energy generation (De Bhowmick et al., 2019).

Fatty acid profiles of the extracted lipids were analysed using GC-MS. Eight identical FAMES with different relative content were found common for ABBR and ABAR (Fig. 3b). Chain length of FAMES was observed between C14 to C20. A typical distribution of sixteen-eighteen carbon fatty acids with no more than three degrees of unsaturation (16–18: ≤ 3), a characteristic of many fresh water green algae, was substantiated. The FAMES as a percentage of the total fatty acids' mixture is displayed in the Table 2. Total fatty acids in ABBR were composed of 31.8% saturated fatty acid (SFA), 11.06% mono-unsaturated fatty acids (MUFAs) and 3.99% polyunsaturated fatty acids (PUFAs), which increased to 46.51% SFA, 20.76% MUFAs and 11.3% PUFAs in ABAR (Fig. 3c). Literature review (Mathimani et al., 2016) has suggested C16 and C18 to be the chief fatty acids in biodiesel. Both ABBR and ABAR observed hexadecanoic acid (C16:0) as the principal fatty acid followed by octadecenoic acid (C18: $\omega 9$). The total percentage of C16 (hexadecenoic acid) and C18 (octadecenoic acid) were found to be more than 50% in the current study. While SFAs have a distinguished cetane number and are more oxidative stable, the MUFAs lower the freezing point and enhance subdued temperature properties of biodiesel (Behl et al., 2019b). Stressful circumstances such as, lower growth temperatures, nutrient deprivation, and variation in the light intensity can alter the FAs constitution of microalgae (Daneshvar et al., 2018a). Little deviations in the FA profiles of both ABBR and ABAR, divulged that FTE can be employed for microalgal growth medium as it reserves the diversity of FAs in the microalgae.

3.6. Chronoamperometric studies

3.6.1. Cyclic voltammetry

To investigate the feasibility of the algal based electrodes (ABBR/ITO and ABAR/ITO) towards photocurrent generation, CV studies were performed. The studies were carried out taking advantage of a report published by Sevda et al., which states the potential of microalgae based bioelectrical systems for bioelectricity production by integrating biomass production and industrial effluent treatment (Sevda et al., 2019). ABBR/ITO, under light irradiation recorded an anodic current (I_{pa}) of 0.57 mA at a voltage (V_{pa}) of 0.37 V and a cathodic current (I_{pc})

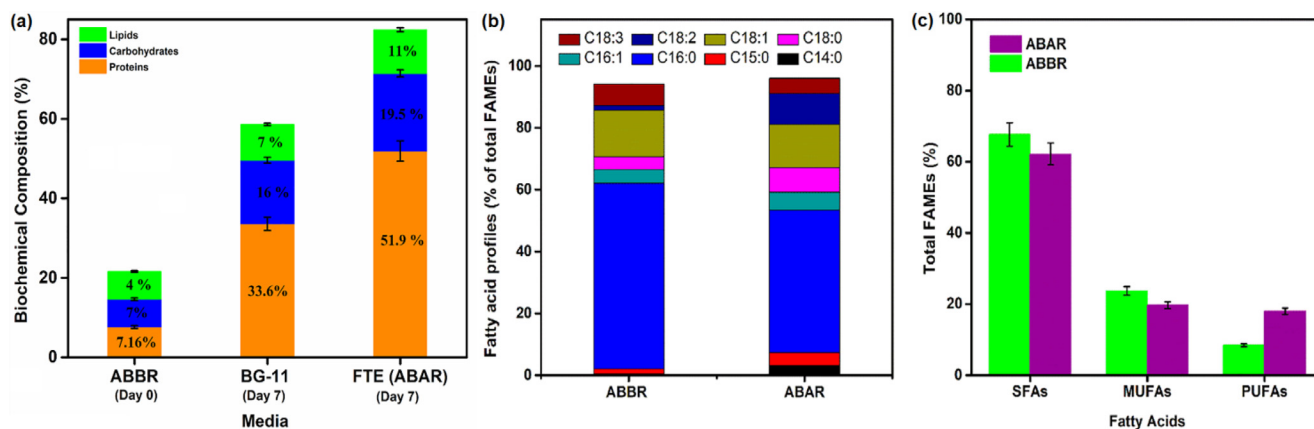


Fig. 3. (a) Biochemical composition of *C. TRC-1* cultivated in BG-11 and FTE after 7 days of cultivation. (b) Fatty acid methyl esters (FAMES) analysis profiles, and (c) FAMES distribution depicting various fatty acids percentage.

of -0.42 mA at a voltage (V_{pc}) of 0.12 V, estimating the potential difference (ΔV) at current positions to be (ΔV) = $V_{pa} - V_{pc} = 0.25$ V (Fig. 4a). However, a decline in the anodic peak (I_{pa} : 0.44 mA, V_{pa} : 0.35 V) and cathodic peak (I_{pc} : -0.35 mA V_{pc} : 0.13 V) was observed, when the ABBR/ITO was kept in dark. A similar peak pattern was also observed in the ABAR/ITO electrode which produced anodic and cathodic peaks at (I_{pa} : 0.82 mA, V_{pa} : 0.51 V) and (I_{pc} : -0.72 mA V_{pc} : 0.01 V), estimating ΔV at current positions to be 0.5 V when kept under light irradiation (Fig. 4b). The peaks, too, observed a downfall in its intensity (I_{pa} : 0.60 mA, V_{pa} : 0.37 V and I_{pc} : -0.49 mA V_{pc} : 0.1 V) when kept under dark.

Green microalgae are photosynthetic chlorophyll containing microorganisms that absorb sunlight and converts it into chemical energy. In the presence of light electrons are generated through photosynthesis as well as respiration. ROS (reactive oxygen species) production and redox reactions are inevitable events that occur in the chloroplasts. Electrons are transported by an electron transport chain from photosystem II (PS II), passing through the PS I system and finally resulting in adenosine-tri-phosphate (ATP) and nicotinamide adenine dinucleotide

phosphate (NADPH) generation (Khetkorn et al., 2017). Simultaneously, oxygen molecules generated in photosynthesis act as electron acceptors at the PS I reducing site, leading to $O_2\cdot$ (Mahler's reaction). The generated $NADP^+$ /ATP and $O_2\cdot$ compete with each other for electrons stemming out of PS I; creating an oxidative stress like situation inside the cell (Robinson & Gibbs, 1982). Thus, for an efficient down regulation of electron transfer in the PS-II and PS-I centres, the electron transporting enzymes (present inside the cell) and the cytochrome proteins (present outside the cell) take part in degenerating the endogenous substances (Valentini et al., 1995). When under stress, the generated electrons from the PS I gets redirected into various sinks (intracellular/extracellular). Moreover, growth is slow in dark and respiratory activities including ATP/NADPH production as well as $O_2\cdot$ generation is lower as compared to light irradiation. Respiration permits the microalgae to survive in dark using nominal energy. In dark, the photosynthetic reactions fix carbon dioxide (CO_2) and reduce it into smaller compounds, either as glycogen or as starch. Utilizing the energy it has accumulated during light reactions, these organic molecules are employed in metabolic activities for internal biological functions

Table 2

Fatty acid methyl esters (FAMES) profiles of ABBR and ABAR of *C. TRC-1*.

Fatty acid			(ABBR)	(ABAR)
Common name	Systematic name	Lipid no.	Total percentage (%)	
<i>Saturated fatty acids (SFAs)</i>				
Lauric acid	Dodecanoic acid	C12:0	1.33	–
Myristic acid	Tetradecanoic acid	C14:0	0.45	3.11
Pentadecyclic acid	Pentadecanoic acid	C15:0	1.57	4.30
Palmitic acid	Hexadecanoic acid	C16:0	60.11	45.96
Margaric acid	Heptadecanoic acid	C17:0	–	0.38
Stearic acid	Octadecanoic acid	C18:0	4.25	7.98
Heneicosylic acid	Heneicosanoic acid	C21:0	–	0.49
<i>Monounsaturated fatty acids (MUFAs)</i>				
ω 7–Palmitoleic acid	(9Z)-Hexadec-9-enoic acid	C16:1	4.43	5.83
ω 9–Oleic acid	(9Z)-Octadec-9-enoic acid	C18:1	14.84	13.92
ω 7–Vaccenic acid	(11E)-Octadec-11-enoic acid	C18:1	3.72	–
Eicosanoic acid	(11Z)-Eicos-11-enoic acid	C20:1	0.78	–
<i>Polyunsaturated fatty acids (PUFAs)</i>				
Conjugated linolenic acid	Hexadecadienoic. Acid	C16:2	–	1.76
ω 6–Linoleic acid	(9Z,12Z)-octadeca-9,12-dienoic acid	C18:2	1.65	9.97
ω 6 – γ –Linolenic acid	all-cis-6,9,12-octadeca-trienoic acid	C18:3	6.87	4.86
ω 3 – α –Linolenic acid	(9Z, 12Z, 15Z)-Octadeca-9,12,15-trienoic acid	C18:3	–	0.99
Eicodienoic acid	(11Z, 14Z)-icosa- 11,14-dienoic acid	C20:2	–	0.45
Σ SFAs			67.71	62.22
Σ MUFAs			23.77	19.75
Σ PUFAs			8.52	18.03
Total			100	100

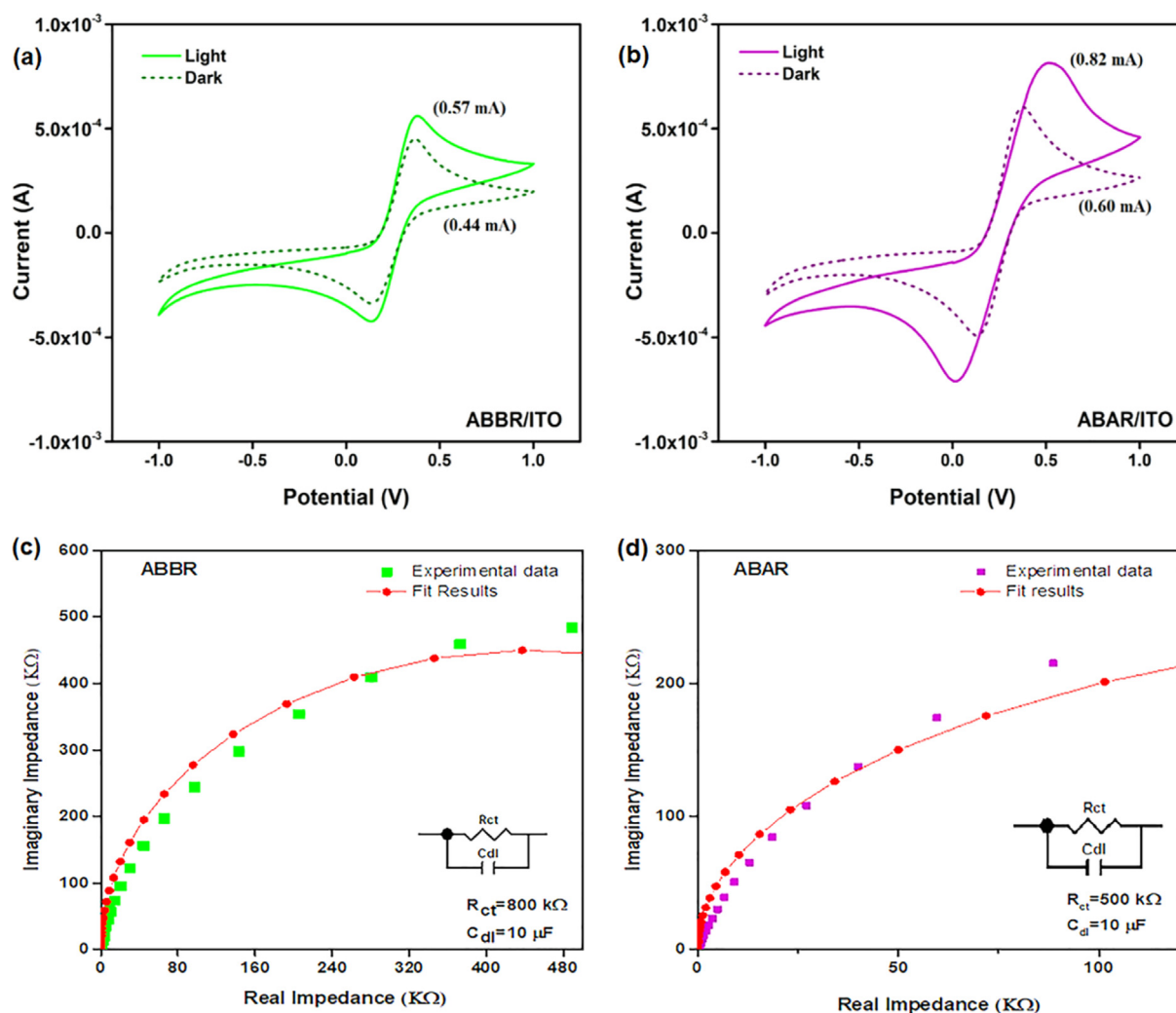


Fig. 4. Cyclic voltammograms scans of (a) ABBR/ITO and (b) ABAR/ITO under light ($100 \mu\text{mol photons m}^{-2}\text{s}^{-1}$; solid line) and dark (dotted line). Representative Impedance spectrum for (c) ABBR, (d) ABAR and fitting results calculated using Electrochemical Impedance Spectroscopy (EIS) Inset: Equivalent circuit model used to extract EIS parameters.

concerning growth and maintenance of the microalgal cell (Furukawa et al., 2006). Ultimately, extracellular electrons (detected in CV scans) are responsible for enhancement in conductivity. Therefore, Chronoamperometric studies using CV confirmed that ABAR/ITO had higher electron generation during light irradiation as well as in dark as compared to ABBR/ITO.

3.6.2. Electrochemical Impedance spectroscopy

EIS analysis was conducted to confirm the resistance in algal based electrodes (ABBR/ITO and ABAR/ITO) by calculating the charge transfer resistance (R_{ct}) at the interface between the electrode and the electrolyte from the EIS curve (Fig. 4c and d). The R_{ct} values decreased from 800 kΩ (ABBR) to 500 kΩ (ABAR). This reduction was observed due to the enhancement in the electron charge transfer between the modified electrodes and the electrolyte. For ABAR, a higher ROS production was observed (supplemented by quantum yield) as compared to ABBR. Under stressful environment, algae rapidly generates electrons (ROS), and quickly redirects it toward various sinks (Meena et al., 2017). This charge transfer may be responsible for higher conductivity or lower resistance. At higher frequencies, the electrodes showed both resistive and capacitive behaviour and at lower frequencies followed a linear line due to the diffusion parameters. These results are in agreement with the CV scans. Thus, chronoamperometric studies using EIS confirmed that ABAR/ITO had lower charge transfer resistance (higher

conductivity) as compared to ABBR/ITO.

The maximum current density after 10 days was observed to be 2.48 A m^{-2} in ABBR while a 50% enhancement in the current density was observed for the ABAR. Similarly, maximum power and power density for ABAR were observed as $4.13 \times 10^{-4} \text{ W}$ and 1.83 W m^{-2} respectively, which is 1.04 times higher than ABBR. (The resistance value for these calculations are approximately in the range of 800 kΩ (ABBR) to 500 kΩ (ABAR)). Enhancement in the conductivity and power generation can be attributed to the abiotic stress conditions (Meena et al., 2017). Tabulated results for current density, power and power density are presented in Table 3.

3.7. Scale-up studies for large scale bioremediation

An experimental system was also fabricated to evaluate the feasibility of *C. TRC-1* for large scale bioremediation. For this purpose,

Table 3

Current density, power and power density of ABBR and ABAR.

Algal Biomass	Current Density (A m^{-2})	Power (W)	Power Density (W m^{-2})
ABBR	2.48	2.05×10^{-4}	1.75
ABAR	3.72	4.13×10^{-4}	1.83

3000 mL treatment chamber was filled with a working volume of 2000 mL FTE and 1 OD algal beads with a flow rate of 5 mL min⁻¹. Residence time in the current study was computed as 400 min (6.67 h) representing that FTE was in contact with the algal beads in the treatment chamber for 400 min. The first cycle was initiated after 6.67 h of residence time. 2000 mL was completely decolorized after 7 days (168 h). Other pollution parameters were also effectively (> 90%) treated within 5 days. The FTE once collected in the collection reservoir was again recycled and filled into the treatment chamber. After the first residence time, 26% dye decolorization was attained and by the 7th day, complete FTE was decolorized. The performance of the experimental set-up was evaluated on the basis of the amount of COD removed (COD_{rem}) during the process. A significant change in the COD_{rem} efficiency (83.07%) was observed during the experimental period of 7 days. The results reflect the applicability of wastewater for biomass production. Simultaneously, the high nitrate (91.75%) as well as phosphate (92.36%) removal were also in agreement with the studies conducted by Sforza et al, which stated, that when the CO₂ supply was limited, microalgae shifted to mixotrophic conditions, utilizing nitrogen and phosphorous for its growth (Sforza et al., 2012).

4. Conclusions

Isolated *C. TRC-1* was able to completely decolorize FTE in 7 days, significantly reducing pollution-indicating parameters. 4% Lipid content increased in spent biomass after FTE remediation and was rich in C16-C18 chain fatty acids (> 90% of total FAMES). Chronoamperometric investigations revealed that spent biomass after FTE biomass had higher electron conductivity and generation under both light (1.43 ×) and dark (1.36 ×). In conclusion, our studies with the newly isolated electrogenic microalgae revealed that *C. TRC-1* could offer a sustainable solution towards environmental bioremediation of textile effluent along with its feasibility for bioelectrode fabrication and as a precursor for biofuel.

CRedit authorship contribution statement

Kannikka Behl: Conceptualization, Methodology, Investigation, Data curation, Writing - original draft. **Pasupuleti Seshacharan:** Methodology, Investigation, Writing - original draft. **Monika Joshi:** Validation, Writing - review & editing. **Mahima Sharma:** Investigation, Data curation, Writing - original draft. **Ashish Mathur:** Formal analysis, Writing - review & editing. **Mukul Suresh Kareya:** Formal analysis, Investigation, Validation, Writing - original draft. **Pannaga Pavan Jutur:** Validation, Writing - review & editing. **Amit Bhatnagar:** Writing - review & editing. **Subhasha Nigam:** Writing - review & editing, Supervision.

Declaration of Competing Interest

The authors declare that they have no known competing financial interests or personal relationships that could have appeared to influence the work reported in this paper.

Acknowledgments

Authors are grateful to the Directors of Amity Institute of Biotechnology and Amity Institute of Nanotechnology, Amity University, Noida, India, for providing the laboratory facilities. Authors thank Mr. Ajay Kumar, AIRF, Jawaharlal Nehru University, for GC-MS. This work was financially supported by a project grant from Department of Science and Technology (DST), Govt. of India, New-Delhi, India, (Sanction no.: DST/TM/WTI/2K16/265). Prof. Amit Bhatnagar acknowledges that his work was partially supported by Nordic Centre of Excellence for Sustainable and Resilient Aquatic Production (SUREAQUA), funded by NordForsk – Norway (Grant

number: 82342), within the Nordic bioeconomy programme.

Appendix A. Supplementary data

Supplementary data to this article can be found online at <https://doi.org/10.1016/j.biortech.2020.122993>.

References

- Ación Fernández, F.G., Gómez-Serrano, C., Fernández-Sevilla, J.M., 2018. Recovery of nutrients from wastewaters using microalgae. *Front. Sustain. Food Syst.* 2 (59).
- Agarwal, A., Patil, S., Gharat, K., Pandit, R.A., Lali, A.M., 2018. Modulation in light utilization by a microalga *Asteracyos sp.* under mixotrophic growth regimes. *Photosynth. Res.* 139, 553–567.
- Ahmad, M., Pataczek, L., Hilger, T.H., Zahir, Z.A., Hussain, A., Rasche, F., Schafleitner, R., Solberg, S.Ø., 2018. Perspectives of microbial inoculation for sustainable development and environmental management. *Front. Microbiol.* 9 2992–2992.
- Aragaw, T.A., Asmare, A., 2018. Phycoremediation of textile wastewater using indigenous microalgae. *Water Practice Technol.* 13, 274–284.
- Asthana, R.K., Srivastava, S., Singh, A.P., Kayastha, A.M., Singh, S.P., 2005. Identification of maltotriose synthase maltotriose trehalose trehalohydrolase enzymes catalysing trehalose biosynthesis in *Anabaena 7120* exposed to NaCl stress. *J. Plant Physiol.* 162, 1030–1037.
- Baker, N.R., 2008. Chlorophyll fluorescence: a probe of photosynthesis in vivo. *Annu. Rev. Plant Biol.* 59 (1), 89–113.
- Behl, K., Sinha, S., Sharma, M., Singh, R., Joshi, M., Bhatnagar, A., Nigam, S., 2019b. One-time cultivation of *Chlorella pyrenoidosa* in aqueous dye solution supplemented with biochar for microalgal growth, dye decolorization and lipid production. *Chem. Eng. J.* 364, 552–561.
- Behl, K., Joshi, M., Sharma, M., Tandon, S., Chaurasia, A.K., Bhatnagar, A., Nigam, S., 2019a. Performance evaluation of isolated electrogenic microalgae coupled with graphene oxide for decolorization of textile dye wastewater and subsequent lipid production. *Chem. Eng. J.* 375, 121950.
- Bligh, E.G., Dyer, W., 1959. A rapid method of total lipid extraction and purification. *Can. J. Biochem. Physiol.* 37 (8), 911–917.
- Bradford, M.M., 1976. A rapid and sensitive method for the quantitation of microgram quantities of protein utilizing the principle of protein-dye binding. *Anal. Biochem.* 72 (1), 248–254.
- Daneshvar, N., Ayazloo, M., Khataee, A.R., Pourhassan, M., 2007. Biological decolorization of dye solution containing Malachite Green by microalgae *Cosmarium sp.* *Bioresour. Technol.* 98 (6), 1176–1182.
- Daneshvar, E., Zarrinmehr, M.J., Hashjin, A.M., Farhadian, O., Bhatnagar, A., 2018c. Versatile applications of freshwater and marine water microalgae in dairy wastewater treatment, lipid extraction and tetracycline biosorption. *Bioresour. Technol.* 268, 523–530.
- Daneshvar, E., Antikainen, L., Koutra, E., Kornaros, M., Bhatnagar, A., 2018a. Investigation on the feasibility of *Chlorella vulgaris* cultivation in a mixture of pulp and aquaculture effluents: treatment of wastewater and lipid extraction. *Bioresour. Technol.* 255, 104–110.
- Daneshvar, E., Zarrinmehr, M., Koutra, E., Kornaros, M., Farhadian, O., Bhatnagar, A., 2018b. Sequential cultivation of microalgae in raw and recycled dairy wastewater: Microalgal growth, wastewater treatment and biochemical composition. *Bioresour. Technol.* 273, 556–564.
- De Bhowmick, G., Sarmah, A.K., Sen, R., 2019. Zero-waste algal biorefinery for bioenergy and biochar: a green leap towards achieving energy and environmental sustainability. *Sci. Total Environ.* 650, 2467–2482.
- El-Batal, A.I., Hashem, A.M., Hassan, M.S., Helal, A.H., 2012. Removal of Dyes from Textile wastewater using treated aspergillus tamarii biomass in batch and column reactor. *World Appl. Sci. J.* 19 (9), 1305–1310.
- El-Naggar, N.E.-A., Hamouda, R.A., Mousa, I.E., Abdel-Hamid, M.S., Rabei, N.H., 2018. Biosorption optimization, characterization, immobilization and application of *Gelidium amansii* biomass for complete Pb²⁺ removal from aqueous solutions. *Sci. Rep.* 8 (1), 13456.
- Empanan, Q., Harun, R., Danquah, M., 2019. Role of phycoremediation for nutrient removal from wastewaters: a review. *Appl. Ecol. Environ. Res.* 17, 889–915.
- Francisco, E.C., Neves, D., Jacob-Lopes, E., Franco, T.T., 2010. Microalgae as feedstock for biodiesel production: carbon dioxide sequestration, lipid production and biofuel quality. *J. Chem. Technol. Biotechnol.* 85, 395–403.
- Furukawa, Y., Moriuchi, T., Morishima, K., 2006. Design principle and prototyping of a direct photosynthetic/metabolic biofuel cell (DPMFC). *J. Micromech. Microeng.* 16 (9), S220–S225.
- Ge, S., Champagne, P., 2017. Cultivation of the marine macroalgae *Chaetomorpha linum* in municipal wastewater for nutrient recovery and biomass production. *Environ. Sci. Technol.* 51 (6), 3558–3566.
- Guldhe, A., Ansari, F.A., Singh, P., Bux, F., 2017. Heterotrophic cultivation of microalgae using aquaculture wastewater: a biorefinery concept for biomass production and nutrient remediation. *Ecol. Eng.* 99, 47–53.
- Gupta, S., Pawar, S.B., Pandey, R.A., 2019. Current practices and challenges in using microalgae for treatment of nutrient rich wastewater from agro-based industries. *Sci. Total Environ.* 687, 1107–1126.
- Han, F., Pei, H., Hu, W., Han, L., Zhang, S., Ma, G., 2016. Effect of high-temperature stress on microalgae at the end of the logarithmic phase for the efficient production of lipid. *Environ. Technol.* 37 (20), 2649–2657.

- Huang, J., Liu, J., Kuo, J., Xie, W., Zhang, X., Chang, K., Buyukada, M., Evrendilek, F., 2019. Kinetics, thermodynamics, gas evolution and empirical optimization of (co-) combustion performances of spent mushroom substrate and textile dyeing sludge. *Bioresour. Technol.* 280, 313–324.
- Huy, M., Kumar, G., Kim, H.-W., Kim, S.-H., 2018. Photoautotrophic cultivation of mixed microalgae consortia using various organic waste streams towards remediation and resource recovery. *Bioresour. Technol.* 247, 576–581.
- Hwang, J.-H., Church, J., Lee, S.-J., Park, J., Lee, W., 2016. Use of microalgae for advanced wastewater treatment and sustainable bioenergy generation. *Environ. Eng. Sci.* 33 (11), 882–897.
- Ji, Y., Hu, W., Li, X., Ma, G., Song, M., Pei, H., 2014. Mixotrophic growth and biochemical analysis of *Chlorella vulgaris* cultivated with diluted monosodium glutamate wastewater. *Bioresour. Technol.* 152, 471–476.
- Khetkorn, W., Rastogi, R.P., Incharoensakdi, A., Lindblad, P., Madamwar, D., Pandey, A., Larroche, C., 2017. Microalgal hydrogen production – a review. *Bioresour. Technol.* 243, 1194–1206.
- Martínez, M.E., Jiménez, J.M., El Yousfi, F., 1999. Influence of phosphorus concentration and temperature on growth and phosphorus uptake by the microalga *Scenedesmus obliquus*. *Bioresour. Technol.* 67 (3), 233–240.
- Mathimani, T., Beena Nair, B., Ranjith Kumar, R., 2016. Evaluation of microalga for biodiesel using lipid and fatty acid as a marker – a central composite design approach. *J. Energy Inst.* 89 (3), 436–446.
- Meena, K.K., Sorty, A.M., Bitla, U.M., Choudhary, K., Gupta, P., Pareek, A., Singh, D.P., Prabha, R., Sahu, P.K., Gupta, V.K., Singh, H.B., Krishanani, K.K., Minhas, P.S., 2017. Abiotic stress responses and microbe-mediated mitigation in plants: the omics strategies. *Front. Plant Sci.* 8, 172.
- Ng, F.-L., Phang, S.-M., Periasamy, V., Yunus, K., Fisher, A., 2017. Enhancement of power output by using alginate immobilized algae in biophotovoltaic devices. *Sci. Rep.* 7, 16237.
- Nigam, S., Rai, M.P., Sharma, R., 2011. Effect of nitrogen on growth and lipid content of *Chlorella pyrenoidosa*. *Am. J. Biochem. Biotechnol.* 7 (3), 124–129.
- Ordoñez, A., Wangpraseurt, D., Lyndby, N.H., Kühl, M., Diaz-Pulido, G., 2019. Elevated CO₂ leads to enhanced photosynthesis but decreased growth in early life stages of reef building coralline algae. *Front. Mar. Sci.* 5 (495).
- Qie, F., Zhu, J., Rong, J., Zong, B., 2019. Biological removal of nitrogen oxides by microalgae, a promising strategy from nitrogen oxides to protein production. *Bioresour. Technol.* 292, 122037.
- Rausch, T., 1981. The estimation of micro-algal protein content and its meaning to the evaluation of algal biomass I. Comparison of methods for extracting protein. *Hydrobiologia* 78 (3), 237–251.
- Rice, E.W., Baird, R.B., Eaton, A.D., Clesceri, L.S., Laura, B., 2012. *Standard Methods: For the Examination of Water and Wastewater*, 22nd ed. United States of America, Washington DC.
- Robinson, J.M., Gibbs, M., 1982. Hydrogen peroxide synthesis in isolated Spinach Chloroplast Lamellae: an analysis of the Mehler reaction in the presence of NADP reduction and ATP formation. *Plant Physiol.* 70 (5), 1249–1254.
- Salama, E.-S., Kabra, A.N., Ji, M.-K., Kim, J.R., Min, B., Jeon, B.-H., 2014. Enhancement of microalgae growth and fatty acid content under the influence of phytohormones. *Bioresour. Technol.* 172, 97–103.
- Sevda, S., Garlapati, V.K., Sharma, S., Bhattacharya, S., Mishra, S., Sreekrishnan, T.R., Pant, D., 2019. Microalgae at niches of bioelectrochemical systems: a new platform for sustainable energy production coupled industrial effluent treatment. *Bioresour. Technol. Rep.* 7, 100290.
- Sforza, E., Simionato, D., Giacometti, G.M., Bertuccio, A., Morosinotto, T., 2012. Adjusted light and dark cycles can optimize photosynthetic efficiency in algae growing in photobioreactors. *PLoS One* 7, e38975.
- Sinha, S., Singh, R., Chaurasia, A.K., Nigam, S., 2016. Self-sustainable *Chlorella pyrenoidosa* strain NCIM 2738 based photobioreactor for removal of Direct Red-31 dye along with other industrial pollutants to improve the water-quality. *J. Hazard. Mater.* 306, 386–394.
- Subashini, P., Raju, R., 2018. An investigation of textile wastewater treatment using *Chlorella vulgaris*. *Orient. J. Chem.* 34, 2517–2524.
- Valentini, R., Epron, D.P.A., Matteucci, G.E.D., 1995. In situ estimation of net CO₂ assimilation, photosynthetic electron flow and photorespiration in Turkey oak (*Q. cerris* L.) leaves: diurnal cycles under different levels of water supply. *Plant, Cell Environ.* 18 (6), 631–640.
- Wu, Y., Li, T., Yang, L., 2012. Mechanisms of removing pollutants from aqueous solutions by microorganisms and their aggregates: a review. *Bioresour. Technol.* 107, 10–18.
- Xu, L., Cheng, X., Wang, Q., 2018. Enhanced Lipid Production in *Chlamydomonas reinhardtii* by Co-culturing With *Azotobacter chroococcum*. *Front. Plant Sci.* 9 741–741.
- Yu, H., Kim, J., Lee, C., 2019. Nutrient removal and microalgal biomass production from different anaerobic digestion effluents with *Chlorella* species. *Sci. Rep.* 9 (1) 6123–6123.